Journal of the Nigerian Association of Mathematical Physics
Volume34,(March, 2016), pp 277 – 286

Removal of Harmonics Flicker Generated by Arc Welding Electronic Machines Using Electronic Filter

[1]Eyenubo O.J., [2]Oniyemofe C.O., [3]Tanno K.O. and [4]Okonye S.

[1,2,&4]Department of Electrical/Electronic Engineering.
[2]Department of Computer Engineering, Delta state Polytechnic, Otefe-Oghara, Delta State, Nigeria.

Abstract

Welding machines are widely used in industry. This type of equipment produces very high disturbances in the low-voltage network, where they are mostly connected. The arc welding machines input current have low frequency oscillations and also a wide-band harmonic spectrum with the presence of interharmonics, which can give rise to flicker. In this paper an electronic welder model is developed. The system simulation is performed so that the voltage harmonic spectrum at the Point of Common Coupling (PCC) is analyzed. The model for a flicker meter is proposed and used in measurements. The flicker level created by the electronic welder is studied and a criterion for further analysis is pointed. Simulation results are presented and discussed.

1.0 Introduction

To achieve a good level of power quality in the three phase electricity supply network, all sources causing significant disturbances must be studied, looking for solutions that can reduce and minimize voltage distortion.

One important group of disturbances generators are the welding machines. Beside other aspects they are large sources for harmonics, interharmonics and sub-harmonics, thereby for flicker (low frequency mains voltage fluctuations). This is caused by the non-linear behaviour of the welding process and also due to the individual welding action varying between a second and several seconds. This voltage fluctuation cause changes in luminance of lamps. At certain oscillation frequencies the flicker becomes annoying, even for voltage fluctuations of very small amplitude. In certain cases interharmonics can also cause interference in ripple control systems. Nowadays, the levels of inter-harmonic voltages have not been thoroughly investigated. These levels are under consideration [1, 2, 3].

Electronic welders, due to their capability for controlling the welding current and the dc voltage and being easily adapted for any kind of welder techniques, are at the moment important sources for flicker generation. The portability of those machines has increased their spread as well as the flicker problem dissemination.

There are several welding processes [4]. In the most common processes a high welding dc current is used with low voltage. In Shielded Metal Arc Welding (SMAW), which is the most popular welding process or in Gas Tungsten Arc Welding (GTAW) also known as TIG (Tungsten Inert Gas), the dc welding current must be controlled.

This dc welding current can also be controlled with a pulsed shape with a frequency varying between *10 Hz* and *300 Hz*. On the high current level penetration and fusion are achieved. The quantity of fusion metal can be adjusted acting in the peak current. On the low current level the work is allowed to cool slightly and so the welding power can becontrolled.

2.0 Harmonics Distortion and Fourier Series

Any periodic (repetitive) complex waveform is composed of a sinusoidal component at the fundamental frequency and a number of harmonic components which are integral multiples of the fundamental frequency. The instantaneous value of voltage for non-sinusoidal waveform or complex wave can be expressed as:

$$\begin{aligned} V &= V_0 + V_1 * \sin(\omega t + \varphi_1) + V_2 * \sin(2\omega t + \varphi_2) + V * \sin(3\omega t + \varphi_3) \\ &+ \cdots + V_n * \sin(n\omega t + \varphi_n) \end{aligned} \tag{2.1}$$

Corresponding author: Eyenubo O.J., E-mail:eyenubo63@yahoo.com, Tel.: +2348167393531

where,

V	=	instantaneous value at any time t
V_0	=	direct (or mean) value (DC component)
V_1	=	rms value of the fundamental component
V_2	=	rms value of the second harmonic component
V_3	=	rms value of the third harmonic component
V_h	=	rms value of the h^{th} harmonic component
$\emptyset_h$	=	relative angular frequency
ω	=	$2\pi f$
f_0	=	frequency of fundamental component ($1/f$ defining the time over which the complex wave repeats itself)

Fourier Series and associated analysis methods introduced by (*Joseph Fourier*, *a 19th century French physicist*) said that any periodic function in interval of time could be expressed by the sum of the fundamental and a series of higher order harmonic frequencies which are integral multiplies of the fundamental component. Ignoring any *DC* components in the above formula, where V_1 and I_1 represent the fundamental voltage and current, respectively, the instantaneous *rms* voltage, V_h, can be represented as a Fourier series. The algorithm called discrete Fourier transform (*DFT*) is used to analyze the frequency content of the time-domain signal. According to the Sampling theorem, the sampling frequency of the data must be at least twice the highest frequency contained in the original signal for a correct transfer of information to the sampled system. The frequency at half the sampling frequency is called *Nyquist frequency*. The effect called "*aliasing*" can happen when the sampling frequency is less than twice the highest frequency present in the sampled waveform. Aliasing causes high-frequency components to appear with genuine low-frequency ones resulting in errors.

The *DFT* of aN-sample sequence can be obtained from equation (2.2).

$$\begin{aligned} C_h &= \frac{2}{N}\sum_{n=0}^{N-1} f[n] * e^{\frac{-j2\pi hn}{N}} \\ &= \frac{2}{N}\sum_{n=0}^{N-1} f[n] * W^{hn} \end{aligned} \qquad (2.2)$$

where,

$h$is the harmonic order, n is the data point number ($n = 0$ represents the 1st data point), N is the total sample points (in 1 cycle) and $W = e^{\frac{-j2\pi}{N}}$

Equation (2.2) can be written in a matrix form as

$$\begin{bmatrix} C_0 \\ C_1 \\ \vdots \\ C_{N-1} \end{bmatrix}_{Nx1} = \frac{2}{N}\begin{bmatrix} W^{(0x0)} & W^{(0x1)} & \cdots & W^{(0x(N-1))} \\ W^{(1x0)} & W^{(1x1)} & \cdots & W^{(1x(N-1))} \\ & & \vdots & \vdots \\ W^{((N-1)x0)} & W^{((N-1)x1)} & \cdots & W^{((N-1)x(N-1))} \end{bmatrix}_{NxN} \begin{bmatrix} f[0] \\ f[1] \\ \vdots \\ f[N-1] \end{bmatrix}_{Nx1}$$

$$\begin{bmatrix} C_0 \\ C_1 \\ \vdots \\ C_{N-1} \end{bmatrix} = \frac{2}{N}\begin{bmatrix} 1 & 1 & \cdots & 1 \\ 1 & W & \cdots & W^{N-1} \\ & & \vdots & \vdots \\ 1 & W^{N-1} & \cdots & W^{((N-1)x(N-1))} \end{bmatrix} \begin{bmatrix} f[0] \\ f[1] \\ \vdots \\ f[N-1] \end{bmatrix} = \frac{2}{N}[D] * \begin{bmatrix} f[0] \\ f[1] \\ \\ f[N-1] \end{bmatrix} \qquad (2.3)$$

Harmonic magnitudes and phase angles can be found from absolute and phase values of complex coefficient $C_h$in equation (2.3).

The most commonly used measure of the quality of a periodic waveform is the total harmonic distortion (*THD*).

THD is defined as the rms square value of the harmonics above fundamental, divided by the rms value of the fundamental. Thus, for current can be defined in the frequency domain in terms of the Fourier series coefficients.

$$v(t) = \sum_{h=2}^{\infty} V_h(t) = \sum_{h=2}^{\infty} 2V_h \sin(h\omega_0 + \phi_h) \qquad (2.4)$$

The rms value of voltage can be expressed as [5]:

$$V_{rms} = \sqrt{\frac{1}{T}\int_0^T V^2(t)dt} = \sum_{h=2}^{\infty} V_h^2 = V_1^2 + V_2^2 + V_3^2 + V_4^2 + \cdots + V_h^2 \tag{2.5}$$

$$I_{rms} = \sqrt{\frac{1}{T}\int_0^T I^2(t)dt} = \sum_{h=2}^{\infty} I_h^2 = I_1^2 + I_2^2 + I_3^2 + I_4^2 + \cdots + I_h^2 \tag{2.6}$$

The root mean square (*rms*) voltage or current for "*total harmonic distortion*", V_{thd}andI_{thd}, respectively can be expressed as:

$$V_{THD} = \sum_{h=2}^{\infty} V_n^2 x100\% = \frac{\sqrt{V_2^2 + V_3^2 + V_4^2 + \cdots V_n^2}}{V_1} x100\% \tag{2.7}$$

$$I_{THD} = \sum_{h=2}^{\infty} I_n^2 x100\% = \frac{\sqrt{I_2^2 + I_3^2 + I_4^2 + \cdots I_n^2}}{I_1} x100\% \tag{2.8}$$

Other simple but practical harmonic formulae include [6]:
Total rms current:

$$I_{rms} = \sqrt{I_{fund}^2 + I_{harm}^2} \tag{2.9}$$

or

$$I_{rms} = I_{fund}\sqrt{1 + \left(\frac{I_{thd}}{100}\right)^2} \tag{2.10}$$

Fundamental current

$$I_{fund} = \frac{I_{rms}}{\sqrt{1 + I_{thd}^2}} \tag{2.11}$$

Total fundamental current distortion:

$$I_{thd(fund)} = \sqrt{\left(\frac{I_{thd}}{I_{fund}}\right)^2 - 1} \tag{2.12}$$

Total Demand Distortion [7]:

$$TDD = \frac{\sqrt{\sum_{h=2}^{\infty} I_h^2}}{I_{load}} = \frac{\sqrt{I_2^2 + I_3^2 + \cdots +_n^{I2}}}{I_1} \tag{2.13}$$

where,

I_{load} = maximum demand load current (fundamental) at the *PCC*

TDD = 'total demand distortion' of current (expressed as measured total harmonic current distortion, per unit of load current; for example, a *30%* total current distortion measured against a load would result *50%* in a *TDD* of *15%*).

The discrete Fourier Transform (*DFT*) is a popular method in the harmonic analysis of electric power system. The amplitude, frequency, and phase of each spectral component can be evaluated by the fast Fourier transform (*FFT*). When the sampling frequency is two times greater than the highest constituent frequency, and the sampling period is an integer multiple of the signal period, the harmonic components can be determined by the *FFT* with high accuracy, efficiency and simplicity.

The power system voltage and current can be expressed as

$$x(t) = \sum_{i=0}^{\infty} A_i Cos(2\pi f_i + \varphi_i) \qquad (2.14)$$

where,

fi, *Ai* and *Φi* are the frequency, amplitude, and phase of the i^{th} harmonic component, respectively. Considering a signal *x(t)* sampled with a sampling period *Ts*, we have the following sequence *x(n)*.

$$\begin{aligned} x(n) &= x(nT_S) \\ &= \sum_{i=0}^{\infty} A_i Cos(2\pi f_i + \varphi_i) \end{aligned} \qquad (2.15)$$

where,

$$\omega_i = 2\pi f_i T_S$$

The discrete Fourier Transform (*DFT*), or the discrete spectrum of the signal, is thus as follows:

$$\begin{aligned} x(e^{j\omega}) = \sum_{i=0}^{\infty} [\frac{A_i}{2} e^{j\varphi_1} \delta(\omega - \omega_1) \\ + \frac{A_i}{2} e^{-j\varphi_1} \delta(\omega - \omega_1)] \end{aligned} \qquad (2.16)$$

A weighting window function *w(n)* is then applied on *x(n)* to truncate the infinite sequence, and the following result is obtained:

$$x_w(n) = x(n)w(n); n = 0,1,..., N-1 \qquad (2.17)$$

Following the product theorem of the Fourier transform, the spectrum of $x_\omega(n)$ is given by

$$X(e^{j\omega}) = X(e^{j\omega}) * W(e^{j\omega})$$

$$= \sum_{i=0}^{\infty} = \sum_{i=0}^{\infty} [\frac{A_i}{2} e^{j\varphi_1} \delta(\omega - \omega_1) + \frac{A_i}{2} e^{-j\varphi_1} \delta(\omega - \omega_1)] \qquad (2.18)$$

where,

$W(\omega)$ is the spectrum of the window function $w(n)$.

Considering the spectrum $X_w = (e^{j\omega})$ sampled with a sampling interval $\Delta\omega = 2\pi / N$, the discrete spectrum $X\,w\,(k)$ is

$$X_w(k) = X_w(e^{j\omega})|_{\omega = k\Delta\omega}$$

$$= \sum_{i=0}^{\infty} \frac{A_i}{2} e^{j\varphi_1} [W(k\Delta\omega - \omega_1) \; ; \; k = 0,1,2,...N-1 \qquad (2.19)$$

$$+ W(k\Delta\omega + \omega_1)$$

Assuming the sampling rate is sufficiently higher than the *Nyquist rate*, and the truncation length of the signal is equal to an integer multiple of the signal period, the amplitude and phase of the k^{th} harmonic from $X_w(k)$ are given as:

$$X_w(k) = \frac{A_0}{2} e^{j\varphi_1} \tag{2.20}$$

Since the picket fence effect and energy leakage of *DFT*, however, the results are not precise and cannot fulfill the requirements of harmonic analysis. To improve the precision of the *DFT* algorithm, the windowed interpolating algorithm was proposed. The interpolation can eliminate the errors caused by picket fence effects [8], and the errors produced by energy leakage can be reduced through signal windowing. Various window functions have been proposed [9, 10] among which the *Hanning window* is a popular one because of its relatively low side lobe amplitudes, fast attenuation, significantly less energy leakage compared with rectangular windows, and the easiness to access. The *Hanning window* is defined as

$$w(n) = 0.5 - 0.5 * Cos\left(\frac{2\pi n}{N}\right); \quad n = 0.1, \ldots N-1 \tag{2.21}$$

and its Fourier transform is

$$W(e^{j\omega}) = 0.5U(\omega) + 0.25[U(\omega - \frac{2\pi}{N}) + U(\omega + \frac{2\pi}{N})] \tag{2.22}$$

where,

$$U(\omega) = e^{j\omega/2} Sin\left(\frac{\omega N}{2}\right) / Sin\left(\frac{\omega}{2}\right) \tag{2.23}$$

After windowing, the spectrum of the sampled sequence $X_w = (e^{j\omega})$ is:

$$\left|X(e^{j\omega})\right|_{\omega = k_{mN}^{2\pi}} \approx \frac{A_m Sin(\pi\delta_m)}{2\delta_m(1-\delta_m^2)\pi} \tag{2.24}$$

$$\left|X(e)\right|_{\omega=(K_m+1)\frac{2\pi}{N}} \approx \frac{A_m Sin(\pi\delta_m)}{2\delta_m(1-\delta_m)(2-\delta_m)\pi} \tag{2.25}$$

Let

$$\beta_m = {\left|X(e)\right|_{\omega=(K_m+1)\frac{2\pi}{N}}} \Big/ {\left|X(e^{j\omega})\right|_{\omega=k_{mN}^{2\pi}}} \tag{2.26}$$

and we have

$$\delta_m = \frac{2\beta_m - 1}{1+\beta_m} \tag{2.27}$$

Thus:.

$$A_m = \left|X(e^{j\omega})\right|_{\omega=k_{mN}^{2\pi}} \frac{2\pi\delta_m(1-\delta_m)}{Sin(\pi\delta_m)} \tag{2.28}$$

$$\varphi_m = angle[\left|X(e^{j\omega})\right|_{\omega=k_{mN}^{2\pi}}] - \delta_m \pi(n-1)/N \tag{2.29}$$

The harmonic analyzing module is coded using a set of functions provided. Measurement of *THD*, (*total harmonic distortions*). Fig. 1 shows from *1st - 13th* waveform and the spectrum of harmonics of signals realized.

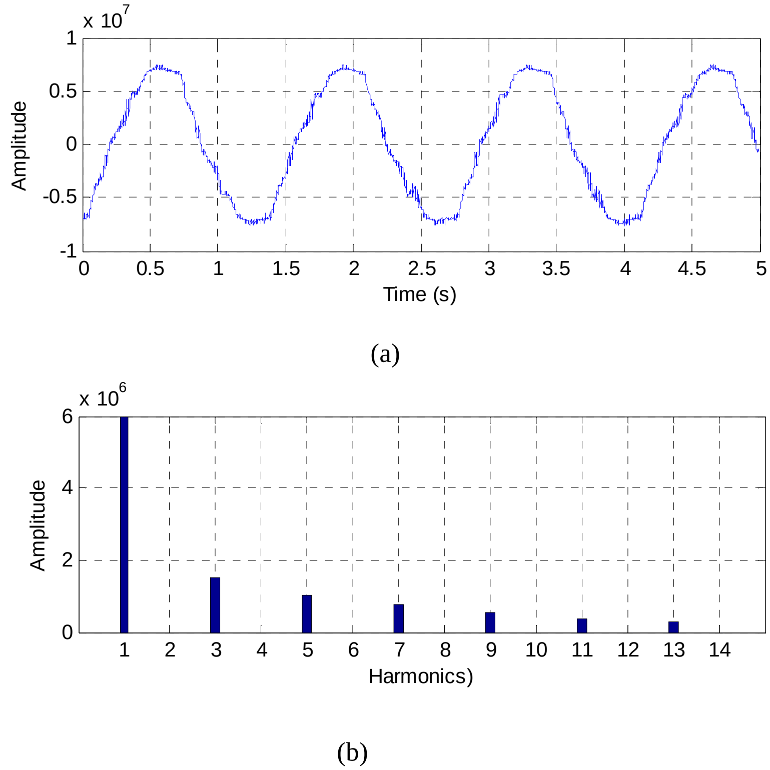

Fig.1: Shows (a) Amplitude of distorted waveform and (b) Harmonic spectrum of the waveform.

There are other processes where a welding dc voltage must be applied like Gas Metal Arc Welding (GMAW) popularly known as MIG (Metal Inert Gas)

There are also mixed processes where dc weldingcurrent control and dc voltage control must be performed alternately, like in Pulsed GMAW. Each control type is selected by an external pulsed wave with a frequency that may vary between *10 Hz* and *300 Hz*.

The two pulsed arc-welding processes mentioned produce even higher disturbances in the ac network. The interaction between the pulse and main frequency generates more interharmonics and sub-harmonics which, depending on their frequencies, can result in annoying values.

2.1 Data Collection

Harmonic data (*voltage and frequency*) were collected form a diesel driven three phase F.G Wilson generator with manufacturer's data as: rated voltage *415/220V*, current *46A* power *32kW, 40 kVA, p.f. 0.8, revolution per minute 1500*sing the necessary measuring tools (*Owon meter/Oscilloscope*). These data were then processed using *Fourier analysis* to ascertain the degree and magnitude of harmonic present in each of these power sources the processed waveform and harmonic *after loading with a non- linear load*.

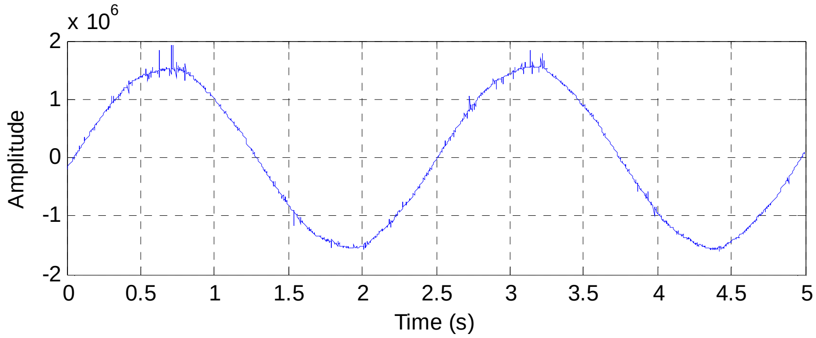

(a)

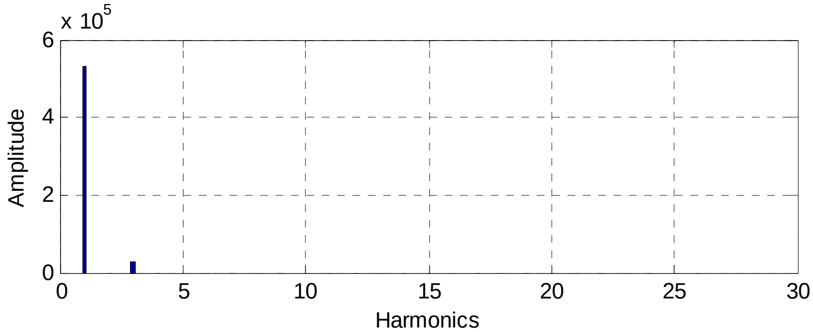

(b)

Fig. 2: Shows (a) processed waveform while(b) spectrum of harmonic before loading with a non- linear load showing the fundamental and the 3rd harmonics.

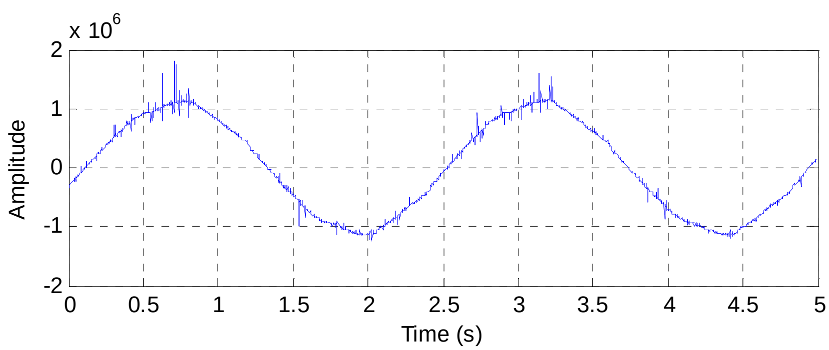

(a)

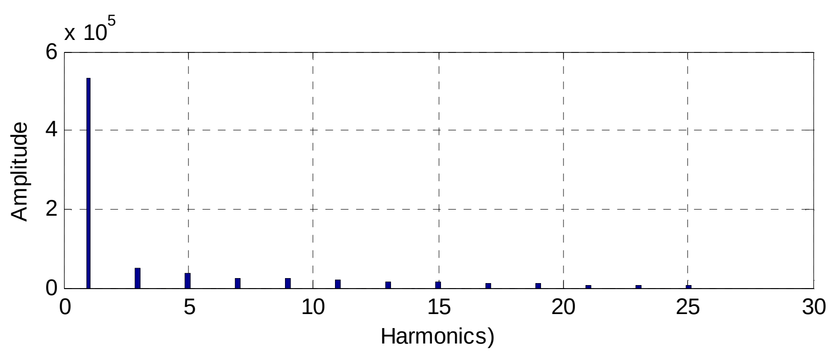

(b)

Fig 3:(a) processed waveform and (b) shows up to 25thharmonic after loading with a non- linear load.

3.0 Development of a Double Tuned Low-Pass Active Shunt Filter Circuit

Assume that this reactive power is to be supplied by the filter circuits, connected to the primary side.

$$MVAR = 2\pi * E^2 * f * C * 10^{-6}$$

$$\therefore C = \frac{MVAR * 10}{2 * \pi * 275 * 275 * 6.0} = 0.935\mu F$$

The harmonics of the order $kp \pm 1$ will be present. So single tuned arms are provided for *the* 5^{th}, 7^{th}, $11^{th}$and 13^{th} harmonics. The fundamental frequency *vars* of a high-pass arm are nearly that due to its capacitor alone (*with remaining components short circuited*). But in the case of single-tuned arms, the voltage at the capacitor terminal is somewhat higher than the system voltage. The relationship for individual harmonics is:

$$\frac{V_{C1}}{V_{n1}} = 1 + \frac{1}{n^2 - 1} \tag{3.1}$$

where,

V_{cl}= fundamental frequency voltage of capacitor
V_{n1} = fundamental frequency system voltage
n = harmonic number. This gives the following numerical values:

when,

$n = 1, 2, 3, 4, 5, 6, 7, 8, 9, 10, 11$

The corresponding values of C, L and R will be computed thus:

$\frac{V_{C1}}{V_{n1}} =$ For various values of n:

Therefore using these values, the capacitance of each arm can be reduced accordingly. We now turn our attention to the design of the inductive and resistance components. The following relationship applies for the value of reactance

$$X_{Ln} = \frac{1}{n^2} X_{nC} \tag{3.2}$$

when,

X_{Ln}= reactance of reactor at fundamental frequency
X_{Cn} = capacitor reactance at the fundamental frequency
n = harmonic number.

$$2\pi f * L = \frac{1}{2\pi f * C}$$

$$L_n = \frac{1}{\omega_n^2 C_n} \tag{3.3}$$

The quality factor of the coil is given by

$$Q = \frac{\omega_n L_n}{R_n} \tag{3.4}$$

where$\omega_n = 2\pi$ * *normal resonance frequency*.
The optimum value of Q as derived as in

$$Q = \frac{1 + Cos\phi_a}{2\delta + Sin\phi_a} \tag{3.5}$$

where,

Φ_a= system impedance angle a
δ = total detuning expected due to all causes.

Assuming the capacitor temperature co-efficient is *0.01 %* per degree C, inductor temperature co-efficient *0.005 %* per degree C, ambient temperature $\pm 2\ 0°C$ and frequency tolerance is *+1 %* then *6 = (0.4 + 0.2 + 1)%= 1.6 %*

$$\therefore Q = \frac{1 + Cos(75.8^0)}{2 * 1.6 * Sin(75.8^0)} x100\% = 41$$

From equations (3.5) will enable the computation of the value of Q, then the R's values can be computed using equation (3.4)

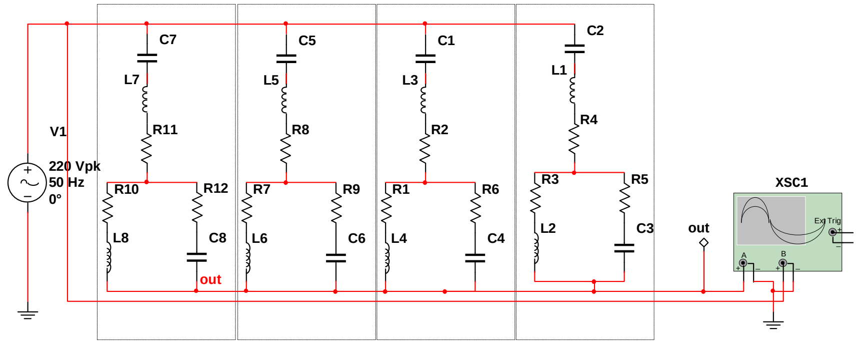

Figure 4:A developed section of double tuned low-passActive shunt filter circuit for simulation.

The developed double tuned low- pass active shunt filter is implemented in Matlab/Simulink environment and will be used for the mitigation of the harmonic data collected from the six power sources investigated.

4.0 Filtered Results

The harmonic filtering capability of the designed double tuned low-pass active shuntfilter was demonstrated in the Matlab/Simulink environment and the corresponding results are as presented

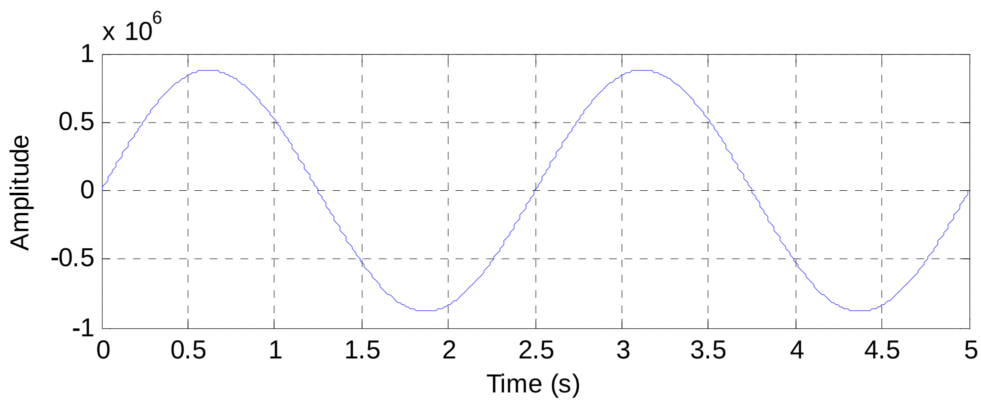

(a)

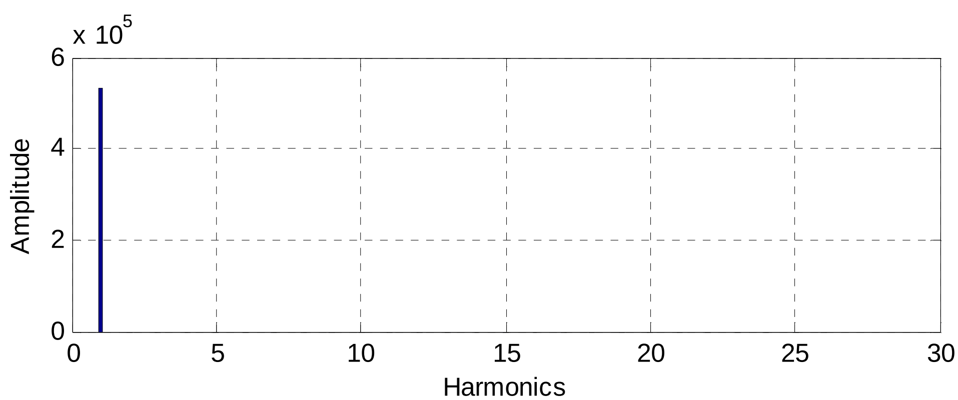

(b)

Fig. 5: Shows (a) and (b) processed waveform after filtering with double tuned low-pass active shuntfilter only the Fundamental spectrum is obtained.

From the power source, the V_{THD} results before filtering using the double tuned low-pass active shuntfilter is*4.321%*and the spectrum has the fundamental and up to the 25^{th} harmonic as shown in Fig.4, but after filtering the V_{THD} *is 1.378%*. The spectrum shows the fundamental harmonic as shown in Fig.5

In the power source investigated the V_{THD} computed for *after filtering*, using the designed filter (*double tuned low-pass active shuntfilter*) falls within the acceptable limit *of 5% as recommended IEEE.*

5.0 Conclusion

In this work it has been demonstrated from measured data that harmonic disturbances with nonlinear loads when compared to power source. An efficient but simple technique have been developed for improving power quality disturbances power sources commonly used in homes by the use of by a double tuned low-pass active shunt filter circuit. The proposed model of the filter which was implemented and simulated in the *MATLAB/Simulink* environment proved to have the capability of effectively reducing the magnitude and frequency of voltage spikes significantly.

6.0 References

[1] European Committee for Electrotechnical Standardization (CENELEC), EN50160, 2004, pp. 709-714.

[2] Huang C.L., Michael E, and Habetler T.G 2001 '*The Mathematics of Circuit Analysis'*, John Wiley and Sons, INC., New York.

[3] Grandke T, 2003, "Interpolating algorithms for discrete Fourier transforms of weighted signals", *IEEE Trans. Instrum.Meas.*, vol.32, pp.350-355.

[4] International Electrotechnical Commission, International Standard IEC 1000-2-1, 2009, pp. 1100-1107.

[5] International Electrotechnical Commission, International Standard IEC 1000-2-2, 2009.

[6] Jain V. K., Collins W. L., and Davis D. C., 2009, "Highaccuracy analog measurements via interpolated FFT", *IEEE Trans. Instrum. Meas.*, vol.28, pp.226-232.

[7] Stinchcomb C., 2009, Welding technology today, principles and practices, Prentice Hall.

[8] Zhang Fu-sheng, GengZhong-xing, Ge Yao-zhong, 2006, "FFT algorithm with high accuracy for harmonic analysis in power system", *Proceedings of the CSEE*, vol.19, no.3, pp.63-66.

[9] Ponomarev V., Scotti A., and ASlivinskiy, 2003, "Atlas of MIG/MAG Welding Metal Transfer Modes", IIW Doc. XII1771 to 1775-03, Bucharest.

[10] Kim, C.H. 2001, "A study of an arc sensor model for gas metal arc welding with rotating arc Part 1: dynamic simulation of wire melting ", Proceedings of the Institution of Mechanical Engineers, Part B: Journal of Engineering Manufacture, Volume 215, Number 9, p. 1271-1279